



Presented at the DLSU Research Congress 2017
De La Salle University, Manila, Philippines
June 20-22, 2017

CFD Verification and Investigation on Building Geometries with BAWT

Jed I. Tapiador^{1*}, Aristotle T. Ubando¹ and Gerardo L. Augusto¹

¹ Mechanical Engineering Department, De La Salle University Manila

*jed_tapiador@dlsu.edu.ph

Abstract: There are emerging studies in wind energy that integrates two buildings with a wind turbine in between. This wind turbine set up is known as a Building Augmented Wind Turbine (BAWT). A verification study was done wherein the building geometries were rectangular in shape with a BAWT in between. This was done by imitating the geometry, meshing, and CFD analysis parameters of a previous study. One reference wind speed and three yaw angles were considered. Results of the verification study showed similar pressure and velocity contours with some deviations at certain areas that interact with the connecting bridge and blade geometry. An investigative study was also done by changing the building geometry to a semi-circular type. One reference wind speed and two yaw angles were considered. Results of the investigation study showed that the semi-circular building geometry yielded slower wind speeds which decreased in the presence of non-zero yaw angles. Structural integrity is a top priority when constructing semi-circular shaped buildings with BAWT due to the presence of compressed turbulence and high pressure difference between the front and back part of the buildings.

Keywords: Computational Fluid Dynamics (CFD); Building Augmented Wind Turbine (BAWT); building geometry; semi-circular building; ANSYS

1. INTRODUCTION

Global energy demand for coal was predicted to slow down within the next five years because of China and United States' shift to renewable energy. The slow shift to renewable energy was aimed in order to improve public air quality and lessen carbon emissions (Chestney, 2016). One form of renewable energy is wind energy wherein kinetic energy from the wind is captured by a rotating turbine to produce electricity. There are emerging studies wherein wind turbines are constructed in between two buildings. This type of wind turbine is known as a Building Augmented Wind Turbine (BAWT). The advantages of using BAWTs are the utilization of wind concentration and visual aesthetics in an urban environment. The main disadvantage of using BAWTs is the incapability to have a yaw drive (Toja-Silva, Comenar-Santos, and Castro-Gil, 2013). In reality, wind changes direction

and magnitude over time. Conventional wind turbines have yaw drives in order to generate optimal energy yield by aligning its blades perpendicular to the wind stream (Mathew, 2006). Therefore, establishing BAWTs cannot generate optimal energy once the wind flows to another direction.

There had been studies which investigated the feasibility of BAWTs in an urban setup. Bayoumi, Fink, and Hausladen (2013) utilized optimization techniques as to the shape of the building façade and placement of BAWTs along the building height. Petkovic et al (2014) investigated different building shapes which would yield higher wind concentration. Indonesian cities were investigated by Sari and Kusumaningrum (2014) wherein future buildings with BAWTs are highly feasible. Bobrova (2015) discussed necessity of efforts coming from both architects and engineers to implement safe, efficient, and visually aesthetic buildings with BAWT. Chaudhry, Calautit,

and Hughes (2015) conducted computational fluid dynamics (CFD) study on the already constructed Bahrain World Trade Centre BAWTs. Their results showed that the BAWTs collect higher energy when receiving wind from the tailwind direction. From the presented literature, wind shear and yaw angle parameters were essential to model BAWTs in order to have realistic results for power and wind velocity. As of this time of writing, there has been no CFD approach to investigate a variety of building geometries including a semi-circular type.

There are minimal literature regarding the study of BAWTs thus this study aims to explore the potential of this technology in order to bring renewable wind energy in an urban setup. A part of this research paper will be a verification study on the work of Heo et al (2016). The goal is to obtain similar pressure and velocity contours of two rectangular buildings with a BAWT. This will be achieved by imitating their simulation set up. When successful verification is done, the research will investigate the pressure and velocity effects of two semi-circular shaped buildings with a BAWT. Pressure and velocity contours will be taken into account in order to see any similarities and differences between the two geometries. Lastly, the velocity of the two setups will be compared to know which geometry yield higher velocity speeds. The commercial CFD software used was ANSYS v.17.1.

2. VERIFICATION STUDY

This part of the research paper will be a verification study on the work of Heo et al (2016). The main objective is to obtain similar pressure and velocity contours of their setup. For simplicity of the verification study, only one wind speed and three yaw angles were considered.

2.1 Geometry and Meshing

Fig. 1 shows the dimensions of the two rectangular buildings with BAWT which is similar to that of the past study. Other unstated dimensions were inferred using ratio and proportion. An oval shaped bridge was used due to the complex design of an elliptical one.

The rotor was an upwind horizontal axis wind turbine. It was modelled with three blades and rotates in a clockwise direction. The blade geometry was procured from Barrett (n.d.). Each blade was angled in order to rotate with the relative velocity of the rotating rotor based from the tutorial by Barrett (n.d.).

Unlike from the past study, the fluid domain used was a box type domain for easier implementation of boundary conditions. The cushion distance of the enclosure are in Table 1. The domain distances were inferred based on the ratio and proportion of the past study.

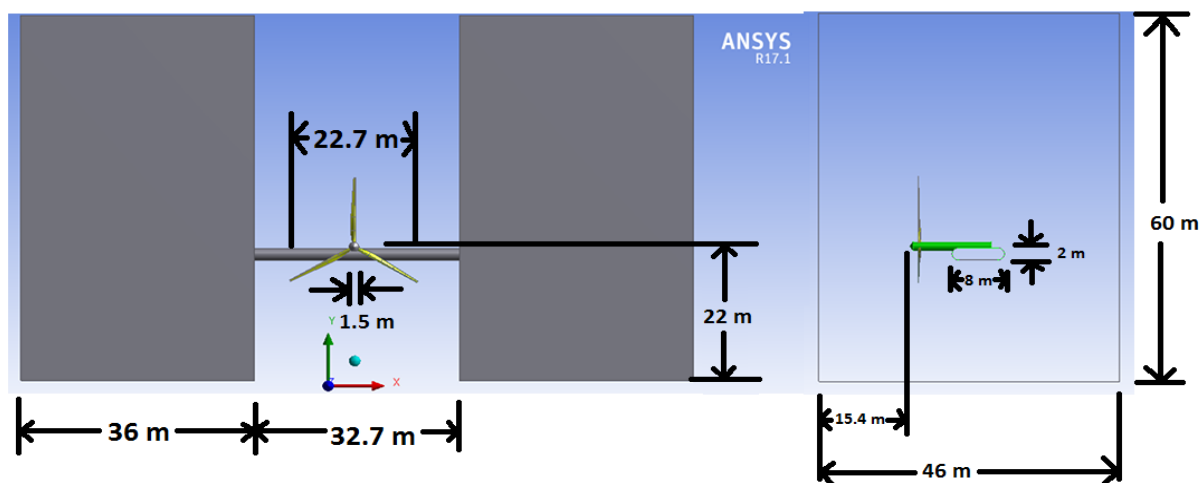


Fig. 1. Dimensions of rectangular shaped buildings with BAWT



Table 1. Cushion Distances of the Fluid Domain

Axis	Distance (m)
+X	
+Y	100
-X	
+Z	240
-Z	
-Y	0.01

Aside from the geometry receiving wind at a yaw angle of 0°, +30° and -30° yaw angles were included in order to deepen the verification.

For the meshing parameters, all elements were in a tetrahedral shape in order to have faster computing time while maintaining reliable results (Chaudhry, Calautit, and Hughes, 2015). Other meshing parameters are stated in Table 2.

Table 2. Meshing Parameters

Parameter	Value
Relevance Center	Medium
Smoothing Setting	Medium
Span Angle Center	Fine

Final meshing resulted into 94,611 nodes and 492,648 elements. The mesh metric showed that the setup had an average skewness of 0.24616, which is considered to be an excellent meshing as stated in ANSYS (2014). Generation of mesh took less than a minute.

2.2 CFD Analysis

Table 3 shows the different parameters and boundary settings used in ANSYS CFX-Pre v.17.1. Wind shear or terrain roughness were considered in the simulation. This is defined as the increase of wind speed as elevation increases due to the absence of physical obstructions that the wind may encounter during its travel (Mathew, 2006).

Table 3. CFD Parameters and Boundary Settings

Parameter	Value
Analysis Type	Steady State
Material	Air at 25°C
Morphology	Continuous Fluid
Reference Pressure	1 atm
Buoyancy Model	Non Buoyant
Domain Motion	Stationary
Inlet Boundary	+Z enclosure plane (in front of BAWT), normal speed equal to Eq. 1.
Outlet Boundary	-Z enclosure plane (behind BAWT), relative pressure of 0 Pa
No Slip Walls	-Y enclosure plane, building surfaces, bridge surfaces, nacelle surface
Free Slip Walls	+Y, +X, and -X enclosure planes

Eq. 1 shows the formula of wind shear that was used similar to the work of Heo et al (2016). The wind shear profile was used in all three yaw angle scenarios.

$$U = U_{ref} \left(\frac{y}{y_{ref}} \right)^{\alpha} \quad (\text{Eq. 1})$$

where:

- U = wind speed at height y , m/s;
- U_{ref} = wind speed at reference height y_{ref} , set to 10m/s;
- y = height or elevation, m;
- y_{ref} = reference height at hub height, m, set to 22m;
- α = power law exponent, set to 0.1 as used by Heo et al (2016).

2.3 Results and Discussion

The solver was set to stop after 100 iterations. Each yaw angle scenario took 100 iterations for 20mins before the solver can complete its task. All solver residuals were below 1.0×10^{-3} .

Fig. 2a shows the horizontal plane of pressure located at the hub height of 22m. The results of this research were highly similar to that of the past study. High pressure was located in front of the buildings. Also, the pressure increases, decreases abruptly, then recovers downstream as it passed through the turbine, which follows the Bernoulli's Principle. The area of low pressure after the blades was lower compared to that of the past study. Furthermore, the low pressure was located just above the bridge.

Fig. 2b shows the vertical plane of pressure located at the middle of the nacelle. The results of this research were different compared to the past study. Although both studies had similar pressure trends before and after the buildings, the pressure varied as it reached the bridge. Significant low pressure was seen surrounding the bridge as indicated by a blue contour. The possible reason for this discrepancy was due to the oval shape of the bridge compared to the elliptical bridge of the past study.

For a yaw angle of 0° , Fig. 3a shows the horizontal plane of velocity. The results of this research were similar to that of the past study but were not exaggerated due to the multiple contour bands allocated. The simulation was able to show higher wind speeds in between buildings due to concentration effect which was represented by the yellow-green color. Just like the past study, axial wind speed was higher on the right side of the BAWT compared to its left side due to the clockwise rotation of the blade. Unlike the past study, noticeable high axial wind speed was seen at the front-top part of the bridge since it contributed to the shearing of wind. Also, it is good to note that there was low axial wind speed few meters in front of the setup which was not captured by the past study.

Fig. 3b shows the vertical plane of velocity. The results of this research did not exactly match that of the past study. Although both studies had similar velocity contour in front of the buildings, the wake of this research did not go upward, but instead went sideward. The results of this research showed

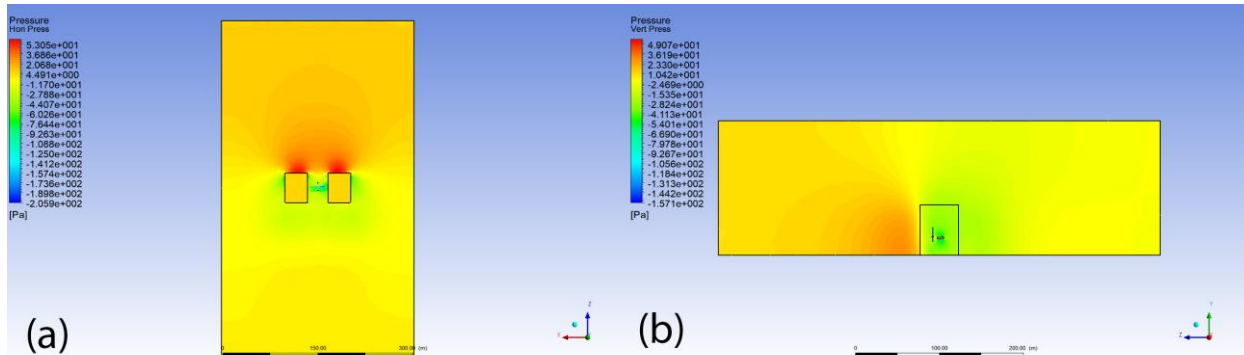


Fig. 2. Horizontal (a) and vertical (b) planes of pressure with wind yaw angle of 0°

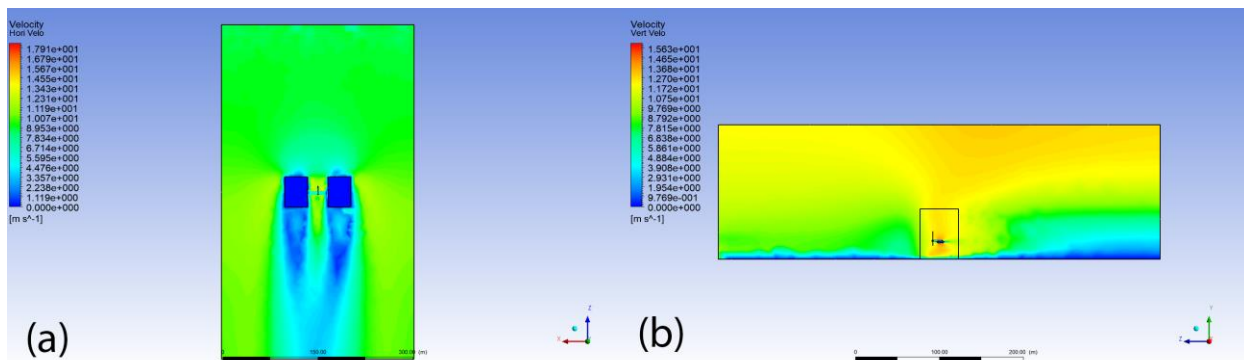


Fig. 3. Horizontal (a) and vertical (b) planes of velocity with wind yaw angle of 0°

that turbulence was developed after the wind passed through the building. High velocity was experienced above the nacelle and below the bridge.

Fig. 4a and 4b shows the horizontal plane of pressure for a yaw angle of $+30^\circ$ and -30° respectively. The results of this research were similar to that of the past study. In both yaw angles, both studies showed a wavelike pressure contour in between the front part of the buildings. Also, the tailwind side of the bridge experienced lesser pressure compared to its headwind side. Unlike the past study, the current research did not show any low pressure field few meters in front of the headwind side of the bridge. High pressure in front of the buildings and Bernoulli's principle were still observed.

The horizontal plane of velocity for both yaw angles of $+30^\circ$ and -30° have symmetrical velocity contours and still displayed wind concentration. Unlike the past study, the $+30^\circ$ did not display a higher axial wind speed compared to its -30° counterpart despite the rotor modelled to rotate clockwise possibly due to the finer mesh of the past study. The vertical plane of velocity for a yaw angle of $+30^\circ$ and -30° showed turbulence forming more near to the buildings.

3. SEMI-CIRCULAR SHAPED GEOMETRY

This part of the study is an investigation of semi-circular shaped geometry buildings with a BAWT. This idea came from the recommendation by Chaudhry, Calautit, and Hughes (2015) after they conducted a CFD verification on the constructed Bahrain World Trade Center. Semi-circular shaped geometries are not common since BAWTs are a

relatively new technology. Therefore, the goal of this part of the paper is to discover the potential of this geometry. The new geometry will be compared and contrasted to the current study's rectangular shaped building.

3.1 Geometry, Meshing, and CFD Analysis

Fig. 5 shows the corresponding dimensions of the new geometry. The height of the buildings was kept at 60m. Wind turbine and bridge dimensions were kept the same.

Meshing set up and techniques were kept the same except mesh relevance set to -10 . Mesh nodes and elements were 91,392 and 478,960 respectively. The mesh is still considered an excellent mesh by ANSYS (2014) with an average mesh skewness of 0.24076.

Same CFD analysis parameters were used in this setup. However, only two yaw angles were considered since -30° yaw angle encountered a solver error regarding domain overflow. The lack of time led to the abandonment of this yaw angle. Therefore, it is assumed that the contours generated by the $+30^\circ$ yaw angle is similar to that of the -30° yaw angle.

3.2 Results and Discussion

The solver was set to stop after 100 iterations. Both yaw angle scenario took 100 iterations for 20mins each before the solver can complete its task. All solver residuals were below 1.0×10^{-3} .

For a yaw angle of 0° , Fig. 6a shows the horizontal plane of pressure. Pressure contour was highly similar to that of Fig 2a. High pressure contour was found at the front part of the semi-circular building. Bernoulli's principle was still observed in the

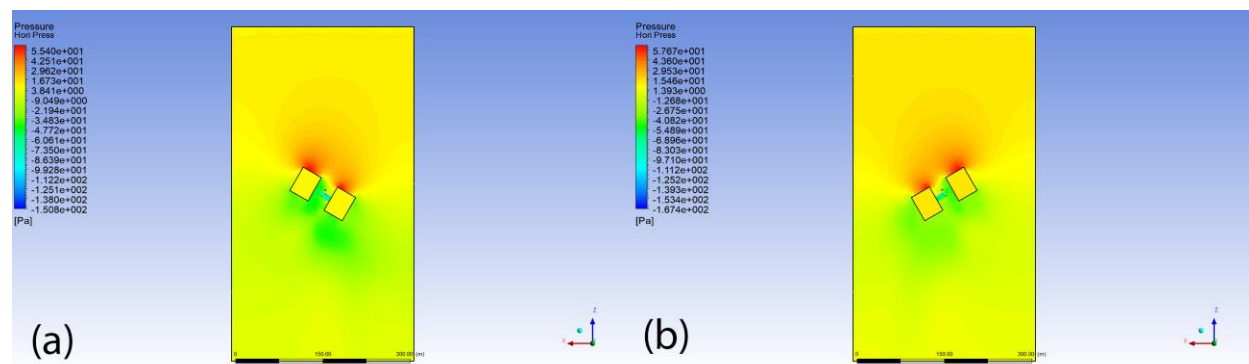


Fig. 4. Horizontal planes of pressure for yaw angle $+30^\circ$ (a) and -30° (b)

setup. A low pressure region was observed at the upper-front part of the bridge.

For a yaw angle of 0° , Fig. 6b shows the vertical plane of pressure. Pressure contour before the BAWT was similar to that of Fig. 2b. Low pressure was also observed surrounding the bridge. For a yaw angle of 0° , the horizontal plane of velocity was similar to that of Fig. 3a. Concentration effect was seen between the two semi-circular buildings. Unlike Fig. 3a, the axial wake profile of the wind moved towards the building's left side. The semi-circular buildings may have effectively concentrate the wind to the clockwise rotation of the rotor which led to the wind wake moving leftward.

Fig. 7a shows the horizontal plane of pressure for a yaw angle of $+30^\circ$. Pressure contour was similar to that of Fig. 4a. Lower pressure was being

experienced on the tailwind side of the bridge compared to its headwind side. High pressure was being experienced at the front part of the buildings. Bernoulli's principle was still observed. However, unlike Fig. 4a, low pressure was observed behind the left building. Therefore, structural integrity must be done in order to protect the building from failure due to this lower pressure being experienced.

Fig. 7b shows the vertical plane of pressure for a yaw angle of $+30^\circ$. The majority of pressure was that of a shade of green, therefore the geometry did not disturb much pressure in the surrounding fluid domain. Higher pressure was experienced at the front part of the building, as indicated by the yellow contour. A vertical oval shaped contour was seen after the BAWT which indicated turbulence.

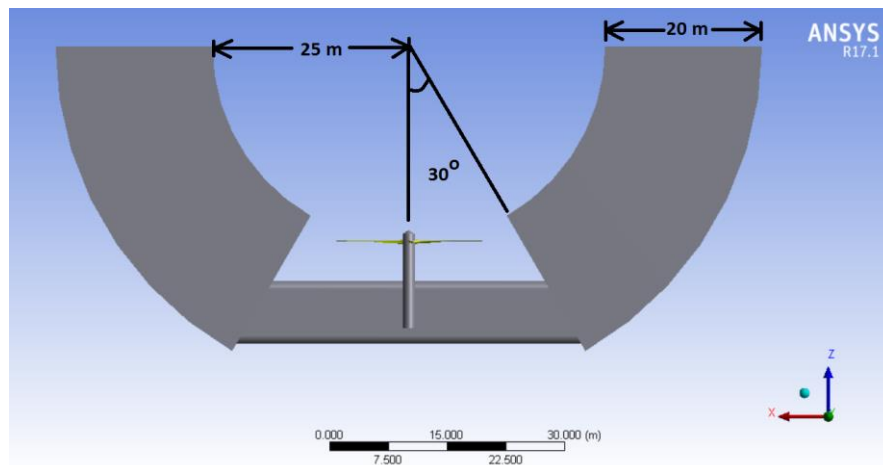


Fig. 5. Dimensions of semi-circular shaped buildings with BAWT

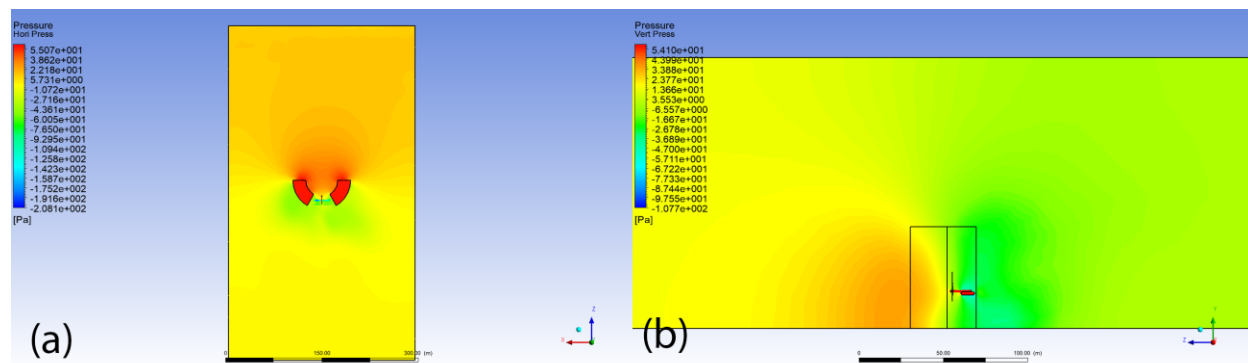


Fig. 6. Horizontal (a) and vertical (b) planes of pressure with wind yaw angle of 0° in investigatory study

Fig. 8a shows the horizontal plane of velocity for a yaw angle of +30°. Concentration effect was still observed. Highest velocity occurred at the front-top part of the bridge. There were higher axial wind speeds behind the left building as seen by the yellow contours.

Fig. 8b shows the vertical plane of velocity for a yaw angle of +30°. Velocity contours were similar to that of the rectangular geometry. Both figures were able to capture turbulence behind the building. However, the turbulence only occurred in a smaller area and more compressed area behind the building.

4. COMPARISON OF TWO GEOMETRIES

The goal of this section is to compare the potential power output of each geometry at various yaw angles. Eq. 2 shows the available power of wind

that a wind turbine can harvest. Due to the cubic relationship between wind velocity and power, small variations in wind velocity would result in significant change in power. The various geometries will be compared through the wind speed hitting the wind blades. Higher velocity is more preferred for a significantly higher power potential.

$$P = \frac{1}{2} \rho A U^3 \quad (\text{Eq. 2})$$

where:

- P = power available in wind stream, W;
- ρ = density of air, kg/m³;
- A = cross-sectional area of rotor, m²;
- U = velocity of wind, m/s (Mathew, 2006);

Table 4 tabulates the wind speed at the tip of the top blade. For the semi-circular geometry, an angled yaw yielded lower wind speed compared to its 0° yaw angle. For a yaw angle of 0°, the rectangular geometry has 15.14% more wind velocity compared to

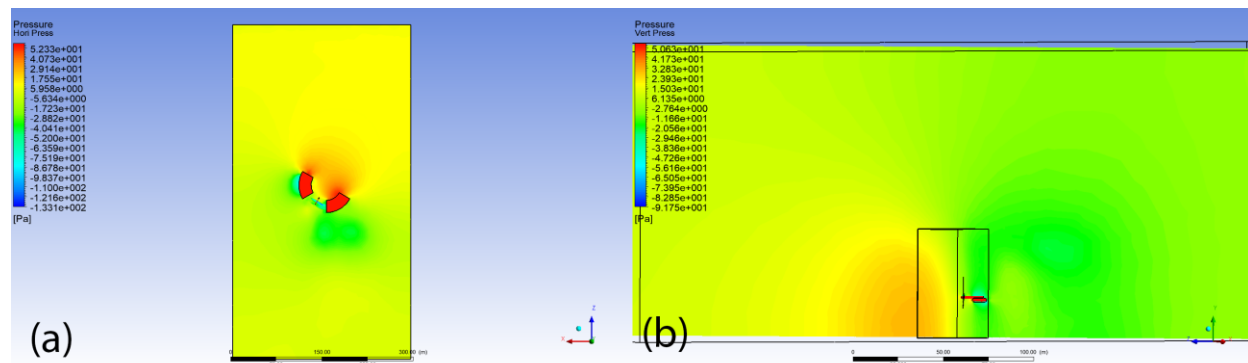


Fig. 7. Horizontal (a) and vertical (b) plane of pressure with wind yaw angle of +30° in investigatory study

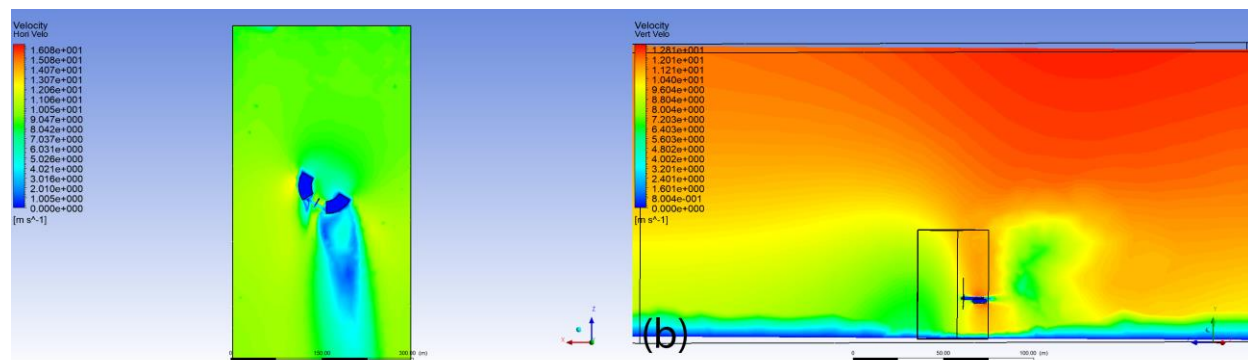


Fig. 8. Horizontal (a) and vertical (b) plane of velocity with wind yaw angle of +30° in investigatory study



its semi-circular counterpart. For a yaw angle of $+30^\circ$, the rectangular geometry has 21.11% more wind velocity compared to its semi-circular counterpart. Due to the cubic relationship of wind velocity and power, the rectangular geometry has 77.64% more energy yield in the $+30^\circ$ yaw angle. Therefore, wind speeds with non-zero yaw angles approaching a semi-circular building will significantly reduce wind speeds being delivered to the rotor. This is due to the turbulence it created behind the buildings which lowered the wind resulting velocity of wind.

Table 4. Velocity Comparison Table

Building Geometry	Yaw Angle ($^\circ$)	Wind Velocity (m/s)
Rectangular	+30	12.5655
	0	12.3981
	-30	12.3600
Semi-Circular	+30	10.3752
	0	10.7680

5. CONCLUSION

A verification study on the work of Heo et al (2016) was conducted by creating similar building geometry, meshing, and CFD analysis. The commercial software used was ANSYS v.17.1. Unstated geometry dimensions were inferred using ratio and proportion. The fluid enclosure was in a shape of a box rather than a cylinder. A wind speed of 10 m/s and yaw angles of $+30^\circ$, 0° , and -30° were only considered for faster verification. The results of this verification study were similar to Heo et al (2016). This present study was able to simulate Bernoulli's principle, high pressure contours in front of buildings, concentration effect, and turbulence formation. However, the verification study did not fully achieve the exact pressure and velocity contours due to the oval shape of the bridge and the type of wind blades used.

An investigative study was also carried out to know the effects of a semi-circular building to the pressure and velocity contours. Identical settings were used in meshing and CFD analysis. A wind speed of 10 m/s and two yaw angles were considered since the -30° yaw angle encountered solver error. Results were

similar to the verification study. However, at the $+30^\circ$ yaw angle, there were lower pressure contours behind the building, higher pressure in front of buildings, lower wind speeds at the building enclosure, and more compressed turbulence after the BAWT. Structural integrity is a high priority to establish safe semi-circular buildings with BAWT.

Both geometries were compared with the velocity speed hitting the turbine blades. Results showed that the rectangular geometry has a better concentration effect compared to its semi-circular counterpart. Furthermore, the semi-circular geometry will have a larger drop of velocity when the wind is not angled at 0° compared to its rectangular counterpart. Therefore, the rectangular shaped geometry yielded better concentration effects and required lesser structural integrity. Investigation of other building geometries is a good recommendation for future studies. Furthermore,

6. ACKNOWLEDGMENT

J.I.T. would like to acknowledge the Engineering Research and Development for Technology (ERDT) consortium and the Department of Science and Technology – Science Education Institute (DOST-SEI) for supporting his academic endeavors in pursuing his Masters in Mechanical Engineering degree.

7. REFERENCES

- ANSYS. (2014). Lecture 8 Mesh Quality. Retrieved March 30, 2017, from http://perso.crans.org/epalle/M2/MFNA/SNECMA_14.5_L08_Mesh_Quality.pdf
- Barrett, S. (n.d.). Wind Turbine Blade FSI (Part 1) - Geometry. Retrieved March 30, 2017, from [https://confluence.cornell.edu/display/SIMULATION/Wind Turbine Blade FSI \(Part 1\) - Geometry](https://confluence.cornell.edu/display/SIMULATION/Wind+Turbine+Blade+FSI+(Part+1)+Geometry)
- Bayoumi, M., Fink, D., & Hausladen, G. (2013). Extending the feasibility of high-rise façade augmented wind turbines. *Energy and Buildings*, 60, 12-19. <http://dx.doi.org/10.1016/j.enbuild.2013.01.013>



Presented at the DLSU Research Congress 2017
De La Salle University, Manila, Philippines
June 20-22, 2017

- Bobrova, D. (2015). Building-Integrated Wind Turbines in the Aspect of Architectural Shaping. *Procedia Engineering*, 117, 404-410. doi:<https://doi.org/10.1016/j.proeng.2015.08.185>
- Chaudhry, H., Calautit, J., & Hughes, B. (2015). Computational Analysis to Factor Wind into the Design of an Architectural Environment. *Modelling and Simulation in Engineering*, 2015. <http://dx.doi.org/10.1155/2015/234601>
- Chestney, N. (2016). Growth In Global Coal Demand To Slow Over Next Five Years: IEA. Retrieved March 25, 2017, from <http://www.reuters.com/article/us-iea-coal-idUSKBN1410WH>
- Heo, Y., Choi, N., Choi, K., Ji, H., & Kim, K. (2016). CFD study on aerodynamic power output of a 110 kW building augmented wind turbine. *Energy and Buildings*, 129, 162-173. <http://dx.doi.org/10.1016/j.enbuild.2016.08.004>
- Mathew, S. (2006). *Wind Energy Fundamentals, Resource Analysis and Economics* (1st ed.). Netherlands: Springer.
- Petkovic, D., Shamshirband, S., Cojbasic, Z., Nikolic, V., Anuar, N., Sabri, A., & Akib, S. (2014). Adaptive neuro-fuzzy estimation of building augmentation of wind turbine power. *Computers & Fluids*, 97, 188-194. <http://dx.doi.org/10.1016/j.compfluid.2014.04.016>
- Sari, D., & Kusumaningrum, W. (2014). A Technical Review of Building Integrated Wind Turbine System and a Sample Simulation Model in Central Java, Indonesia. *Energy Procedia*, 47, 29-36. doi:<https://doi.org/10.1016/j.egypro.2014.01.193>
- Toja-Silva, F., Colmenar-Santos, A., & Castro-Gil, M. (2013). Urban Wind Energy Exploitation Systems: Behaviour Under Multidirectional Flow Conditions—Opportunities And Challenges. *Renewable and Sustainable Energy Reviews*, 24, 364-378. <http://dx.doi.org/10.1016/j.rser.2013.03.052>